Inhibition of Phosphatidylinositol 3-Kinase Destabilizes Mycn Protein and Blocks Malignant Progression in Neuroblastoma

Louis Chesler,[1,2] Chris Schlieve,[2] David D. Goldenberg,[1] Anna Kenney,[6] Grace Kim,[3] Alex McMillan,[4] Katherine K. Matthay,[2] David Rowitch,[6] and William A. Weiss[1,2,5]

Departments of [1]Neurology, [2]Pediatrics, [3]Pathology, and [4]Biostatistics Core, Comprehensive Cancer Center, and [5]Department of Neurological Surgery, University of California at San Francisco, San Francisco, California and [6]Dana-Farber Cancer Institute, Boston, Massachusetts

Abstract

Amplification of *MYCN* occurs commonly in neuroblastoma. We report that phosphatidylinositol 3-kinase (PI3K) inhibition in murine neuroblastoma (driven by a tyrosine hydroxylase-*MYCN* transgene) led to decreased tumor mass and decreased levels of Mycn protein without affecting levels of MYCN mRNA. Consistent with these observations, PI3K inhibition in *MYCN*-amplified human neuroblastoma cell lines resulted in decreased levels of Mycn protein without affecting levels of MYCN mRNA and caused decreased proliferation and increased apoptosis. To clarify the importance of Mycn as a target of broad-spectrum PI3K inhibitors, we transduced wild-type *N-myc* and *N-myc* mutants lacking glycogen synthase kinase 3β phosphorylation sites into human neuroblastoma cells with no endogenous expression of myc. In contrast to wild-type *N-myc*, the phosphorylation-defective mutant proteins were stabilized and were resistant to the antiproliferative effects of PI3K inhibition. Our results show the importance of Mycn as a therapeutic target in established tumors *in vivo*, offer a mechanistic rationale to test PI3K inhibitors in *MYCN*-amplified neuroblastoma, and represent a therapeutic approach applicable to a broad range of cancers in which transcription factors are stabilized through a PI3K-dependent mechanism. (Cancer Res 2006; 66(16): 8139-46)

Introduction

Neuroblastoma, a tumor of peripheral neural crest origin, is the most common extracranial solid tumor of childhood and the third most common pediatric cancer, causing 8% to 10% of all infant malignancies and 15% of cancer-related deaths in children (1). Approximately half of patients present with high-risk disease characterized by unresectable primary lesions and multiple metastases (1). These patients have resisted improvements in multimodal therapy, which in most high-risk patients is complicated by eventual relapse (2).

One third of neuroblastoma tumors show amplification of *MYCN*, a mutation linked to aggressive biological behavior and poor clinical outcome. Amplification of *MYCN* correlates with increased metastases and chemotherapy resistance (3, 4). Neuroblastoma cell lines with amplification of *MYCN* show increased proliferation, down-regulation of angiogenesis inhibitors, inhibition of terminal differentiation, and increased invasive potential (5–12). That amplification and overexpression of *MYCN* play a critical role in the malignant progression of neuroblastoma is further supported by observations that a tyrosine hydroxylase-*MYCN* (TH-*MYCN*) transgene targeted to the murine peripheral neural crest led to tumors with biological and genetic features of high-risk neuroblastoma (13–15).

Given the prominent role of *MYCN* amplification in high-risk neuroblastoma and the limited expression of this gene in other postnatal tissues (16–18), Mycn (protein) represents an ideal candidate for targeted therapy. The ability to inhibit Mycn in patients, however, still presents a formidable challenge. In contrast to small-molecule inhibitors of kinases active in cancer, there is little precedent for orally available small molecules that selectively target transcription factors.

We report here that small-molecule inhibitors of phosphatidylinositol 3-kinase (PI3K) signaling blocked growth of neuroblastomas in mice transgenic for TH-*MYCN* and induced cell cycle arrest and apoptosis in human neuroblastoma cells amplified for *MYCN*. We show that Mycn protein is stabilized through PI3K signaling and that inhibition of PI3K represents an effective strategy to promote degradation of Mycn protein *in vivo* and *in vitro*. These results confirm the importance of Mycn as a therapeutic target in neuroblastoma and suggest that small-molecule inhibitors of PI3K are worthy of further evaluation in clinical trials.

Materials and Methods

***In vivo* therapy in mice transgenic for TH-*MYCN*.** Animals with palpable tumors (~60 days of life) were treated daily with i.p. injections of LY294002 (50 mg/kg in 100 μL DMSO) or vehicle (DMSO) for 12 days. At sacrifice, tumors were excised, measured, weighed, and snap frozen. Tumors were homogenized in TBS with protease inhibitors (Compleat, Roche, Inc., Indianapolis, IN) and lysed as detailed below. Significance analysis was done using the Student's *t* test. All animals were handled in accordance with institutional guidelines for safe and ethical treatment of mice.

Immunoblotting and immunoprecipitation. For immunoblotting, cells were suspended in nondenaturing lysis buffer (Cell Signaling Technology, Danvers, MA) with 0.5% SDS. Lysates were sonicated and cleared at 14,000 × *g* at 4°C. Protein content was assayed by BCA method (Pierce, Rockford, IL), and protein (20-40 mg) was analyzed on 4% to 12% gradient denaturing gels (Invitrogen, Carlsbad, CA). Membranes were incubated overnight at 4°C with primary antibodies [Mycn (Calbiochem, San Diego, CA), phosphorylated T58 c-myc (Cell Signaling Technology), phosphorylated S473 Akt (Cell Signaling Technology), Akt (Cell Signaling Technology), phosphorylated glycogen synthase kinase 3β (GSK3β; Cell Signaling Technology), and β-tubulin (Upstate, Charlottesville, VA)] and then developed using horseradish peroxidase–conjugated secondary antibodies (Calbiochem) and Enhanced Chemiluminescence Plus reagents (Amersham, Pittsburgh, PA). Cycloheximide pulse-chase studies were used

Note: Supplementary data for this article are available at Cancer Research Online (http://cancerres.aacrjournals.org/).

Requests for reprints: Louis Chesler, Pediatric Hematology Oncology, Department of Pediatrics, University of California at San Francisco, Room U-441K, 533 Parnassus Avenue, San Francisco, CA 94143. Phone: 415-502-1695; Fax: 415-476-0133; E-mail: cheslerl@peds.ucsf.edu.

doi:10.1158/0008-5472.CAN-05-2769

to evaluate Mycn protein half-life in the absence of new protein synthesis. Cells were pretreated with LY294002 at various doses. At prescribed intervals, 25 μmol/L cycloheximide was added in pulses of 15 minutes to 6 hours. Cell lysates were then prepared for immunoblotting.

Cell culture and reagents. SH-SY5Y, LAN-1, Kelly, SK-N-SH, and SHEP neuroblastoma tumor cell lines were obtained from the University of California at San Francisco Cell Culture Facility (San Francisco, CA) and from the American Type Culture Collection (Manassas, VA). KCNR cells were generously provided by Pat Reynolds (Children's Hospital, Los Angeles, CA) and Tet21/N cells (19) were a gift from Jason Shohet (Baylor University, Houston, TX). Cells were grown in RPMI or DME with 10% fetal bovine serum (FBS). In some experiments, cells were synchronized by serum starvation in 0.2% FBS for 24 hours before analysis. Where indicated, cells were treated with recombinant human insulin-like growth factor-I (IGF-I; Calbiochem) at 20 to 40 ng/mL for 1 to 6 hours before harvesting. LY294002 (LC Labs, Woburn, MA) was dissolved at 10 to 20 mmol/L in DMSO and stored at −20°C. Lactacystin and GSK inhibitor II were purchased from Santa Cruz Biotechnology (Santa Cruz, CA). Cycloheximide was purchased from Sigma (St. Louis, MO). GSK3β small interfering RNA (siRNA) was from Ambion (Austin, TX). Transient transfection of constructs wild-type or mutant for *N-myc* (Fig. 4) was done using LipofectAMINE 2000 (Invitrogen) in six-well plates. Proteins were harvested at 48 hours.

Proliferation, toxicity, apoptosis assays, and flow cytometry. Assessment of cell growth and proliferation was done by hemacytometer and trypan blue exclusion analysis and by water-soluble tetrazolium (WST-1) 96-well spectrophotometric assay (Roche). In this assay, $A_{450\ nm}$-$A_{690\ nm}$ is proportional to secreted WST-1 activity and proliferation. Maximal absorbance and linearity of the assay was calibrated to cell numbers of 20 to 60,000. Cell necrosis and apoptosis (Figs. 3 and 4) were assessed using a Cell Death Detection ELISA (Roche) that detects intracellular (apoptosis) or released (necrosis) nucleosome-associated histone H2b DNA. Background values were corrected for vehicle (DMSO) control, which in no case exceeded 2% of the total assay value. Cells were plated in 10% FBS at 20 to 60,000/mL in 96-well microplates and assayed at 6 to 24 hours using a Synergy HT-1 multiplate spectrophotometer/luminometer (Bio-Tek, Winooski, VT) at a sensitivity setting of 155, with automatic background correction to the reference wavelength. For the histone ELISA, the readout was $A_{405\ nm}$-$A_{490\ nm}$. Percent toxicity was standardized to the effect of Triton X-100 as a positive control (0-100 μmol/L) with maximal toxicity defined as the plateau absorbance.

Apoptosis was also assessed by terminal deoxynucleotidyl transferase–mediated dUTP nick end labeling (TUNEL) staining using a DEADEnd fluorometric assay kit (Promega, Madison, WI). Cells were plated on coverslips at 50% density and assayed at 24 hours in 10% FBS. For three separate experiments, *P*s were derived from NIH Image spot counts of five high-power fields. The mean difference was calculated using the Student's *t* test. Values were standardized to the maximal effect of camptothecin (5 g/mL). An alternate apoptosis assay used fluorometric detection of an enzymatic substrate specific for cleaved caspase-3 (Caspoglow fluorometric assay kit, Biovision, Mountain View, CA). Cells were plated at 75% density in 24-well plates and grown in 10% FBS. Caspase-3 activity was detected 6 hours after LY294002 treatment according to manufacturer's instructions.

Bromodeoxyuridine (BrdUrd) incorporation in transfected SHEP cells was assessed by flow cytometry. SHEP cells were transfected with *N-myc* constructs or a pWZL-GFP control vector for 24 hours. After drug treatments, cells were pulsed with 25 μg BrdUrd/mL (2 hours), fixed in

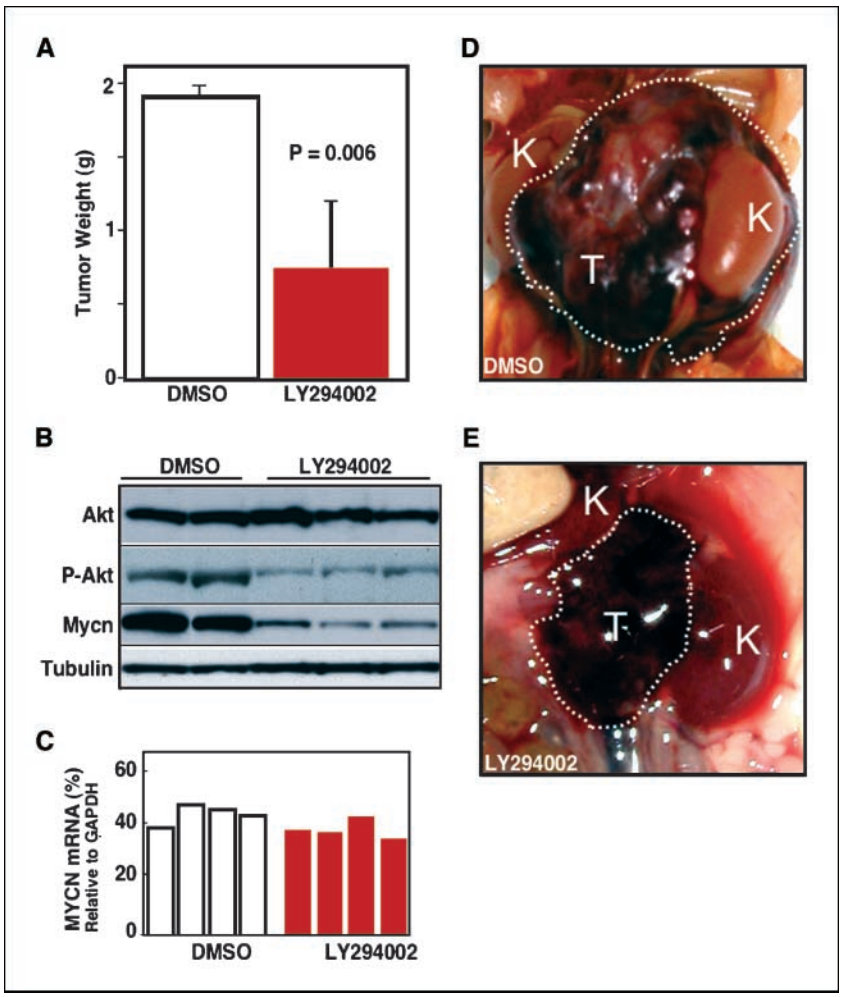

Figure 1. Inhibition of PI3K blocks growth of neuroblastoma *in vivo*. Tumor-bearing animals transgenic for TH-*MYCN* were treated at ~60 days of life using 50 mg/kg LY294002 ($n = 7$) or vehicle ($n = 6$). Treatment was by daily i.p. injection for 12 days, at which time animals were sacrificed. *A,* average weight of resected tumors. *B,* Western analysis of five separate tumors shows decreased levels of Mycn and pAkt in tumor lysates from treated animals. *C,* quantitative reverse transcription-PCR (RT-PCR; Taqman) analysis of MYCN mRNA levels from four tumors treated with LY294002 or vehicle shows no significant differences in levels of MYCN mRNA (43.4% versus 38.7% of GAPDH expression; $\chi^2 = 0.138$; $P \leq 1$). *D,* tumor from a representative animal treated with DMSO, showing a large abdominal primary tumor (*T*) encapsulating one kidney (*K*). *E,* tumor from a representative animals treated with LY294002, showing shrinkage of tumor, with a more discrete primary tumor mass adjacent to the kidney.

40% ethanol, treated with 2 N HCl, incubated with FITC-conjugated anti-BrdUrd (PharMingen, San Diego, CA), and analyzed by flow cytometry using a FACScan with CellQuest acquisition software (Becton Dickinson, San Jose, CA). Each experimental value represents the average of three separate data points per experiment, and data are normalized to incorporation of BrdUrd by a control transfected pWZL-GFP plasmid (fold = 1).

Real-time PCR analysis. Expression of MYCN mRNA was analyzed quantitatively in neuroblastoma cell lines and murine tumors using an ABI7700 Prism instrument as described (20). RNA was prepared using RNeasy mini kits (Qiagen, Valencia, CA), incorporating a QIAshredder step for the murine tumors. Fluorogenic probes for MYCN and β_2-microglobulin were 5′-CGCTTCTCCACAGTGACCACGTCG-3′ and 5′-TGCCTGCCGTGTGAACCATGTGAC-3′, respectively. Gene-specific probes for MYCN mRNA were forward 5′-CGACCACAAGGCCCTCAGTA-3 and reverse 5′-CAGCCTTGGTGTTGGAGGAG-3′. Relative expression of MYCN was derived from $\log_2$ ratios of the C_t values compared with a β_2-microglobulin control and computed as fold differences between the two values. MCM7 probes were from ABI (Foster City, CA). Fluorogenic probe for MDM2 was 5′-CAGTGAATCTACAGGGACGCCATCGAAT-3′. Gene-specific probes for MDM2 were forward 5′-GCCTGGCTCTGTGTGTAATAAGG-3′ and reverse 5′-TGAATCCTGATCCAACCAATCA-3′. Assay controls and method were as described above.

Results

PI3K blockade inhibits growth of established neuroblastoma tumors *in vivo*. We used the PI3K inhibitor LY294002 to treat murine neuroblastoma driven by a TH-*MYCN* transgene (13). Animals with established tumors were treated with LY294002 ($n = 7$) or DMSO vehicle ($n = 6$) daily for 12 days and then sacrificed (Fig. 1*A*). Tumor mass in animals treated with LY294002 was decreased significantly in comparison with vehicle controls ($P = 0.006$). Levels of Mycn and phosphorylated Akt (pAkt) proteins were much lower in treated animals relative to vehicle controls (Fig. 1*B*). The small decrease in MYCN mRNA levels in LY294002-treated tumors (Fig. 1*C*) was not significant statistically [43.4% versus 38.7% relative to glyceraldehyde-3-phosphate dehydrogenase (GAPDH) expression; $\chi^2 = 0.138$; $P \leq 1$], suggesting that PI3K inhibition blocked *MYCN* at a post-transcriptional level. Representative images of vehicle and LY294002-treated tumors are shown in Fig. 1*D* and *E*. Collectively, these data show that PI3K blockade affects Mycn protein and that this therapy can arrest growth of established tumors *in vivo*.

Inhibition of PI3K decreases Mycn in human neuroblastoma cells. To establish the relevance of this approach to human neuroblastoma, we tested the effect of LY294002 in three human neuroblastoma cell lines (Fig. 2). Kelly and LAN-1 are *MYCN*-amplified cell lines expressing high levels of Mycn protein. Tet21/N is an established line stably transfected with a *MYCN* expression construct, in which addition of doxycycline blocks transcription of *MYCN* (19). SH-SY5Y is a derivative of SK-N-SH, expressing high-levels of Mycn, and is unique in its ability to survive under serum-free conditions (21). This line was used to assess the effect of LY294002 in serum-starved cells, where addition of IGF-I is known to induce increased levels of Mycn protein (22).

First, we showed that LY294002 treatment, at doses that blocked activation of pAkt (Supplementary Fig. S1*A*), reduced steady-state levels of Mycn protein (Fig. 2*A*). Cells were grown in 10% FBS, and levels of Mycn protein were assessed 24 hours after addition of LY294002 (20 μmol/L). Figure 2*B* shows that under these treatment conditions mRNA expression was not significantly altered, arguing that LY294002 treatment blocks *MYCN* post-transcriptionally. Collectively, these data show that LY294002 treatment reduces

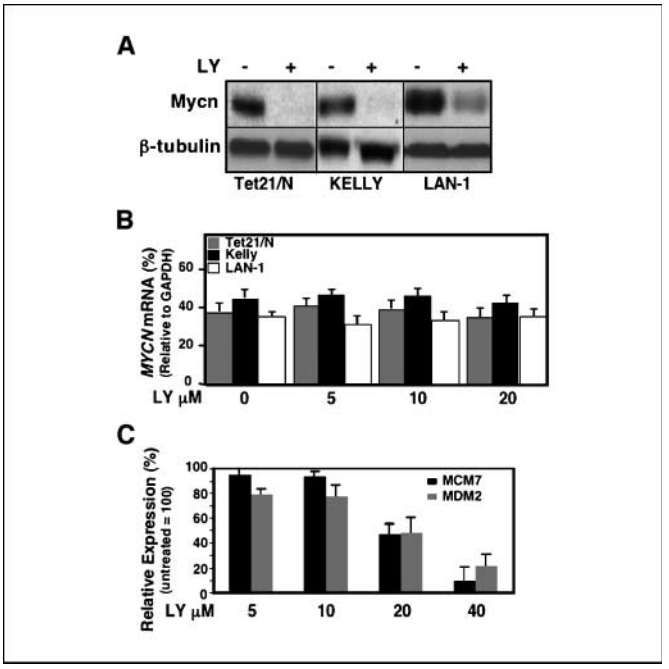

Figure 2. LY294002 treatment reduces steady-state levels of Mycn protein in human neuroblastoma cells. *A,* to assess the effect of LY294002 (*LY*) on steady-state levels of Mycn, neuroblastoma cell lines were grown in 10% FBS and treated with LY294002 (20 μmol/L) for 24 hours. Lysates were immunoblotted with antisera against Mycn protein or β-tubulin. Tet21/N cells are a derivative of SHEP neuroblastoma cells that stably express *MYCN* under control of the tetracycline system. Kelly and LAN-1 are tumor-derived cell lines amplified for *MYCN*. *B,* quantitative RT-PCR (Taqman) analysis of MYCN mRNA levels from Tet21/N, Kelly, and LAN-1 cells treated in (*A*) showed no significant effect of LY294002 on MYCN mRNA expression. Average of three separate conditions. *C,* LY294002-induced destabilization of Mycn was associated with inhibition of the known downstream Mycn targets MDM2 (23) and MCM7 (24). Levels of these targets were assessed by Taqman analysis under the same experimental conditions as in (*A*).

steady-state levels of Mycn protein. To verify that Mycn degradation affected known transcriptional targets, we showed that LY294002-mediated decreases in Mycn protein were associated with concomitant decreases in the levels of two established Mycn targets, MDM2 (23) and MCM7 (24). In Kelly cells grown and treated under the same experimental conditions as in Fig. 2*A*, mRNA levels for both targets were decreased by treatment with LY294002 (20 μmol/L for 24 hours; Fig. 2*C*). Similar data were shown for LAN-1 and SH-SY5Y cells (data not shown).

We next showed that LY294002 blocked the increase in Mycn protein levels observed after addition of IGF-I (in serum-starved SH-SY5Y cells). Control cells treated with IGF-I showed a 4-fold increase in Mycn protein at 6 hours (Supplementary Fig. S1*B*, lane 2), likely a combined result of stimulation of new protein synthesis and PI3K-mediated stabilization of Mycn protein. Treatment with LY294002 blocked this increase (compare lanes 1 and 3), with no effect on levels of MYCN mRNA by Taqman analysis (data not shown).

PI3K blockade inhibits neuroblastoma cells. Having established that PI3K inhibition leads to decreased levels of Mycn protein, we next examined the effect of this treatment on the accumulation of viable cells. The effects of LY294002 are likely to proceed through both Mycn-dependent and Mycn-independent pathways. We therefore assessed the effect of PI3K inhibition in *MYCN*-amplified neuroblastoma cells and in neuroblastoma cell lines expressing little or no Mycn protein. LY294002 reduced the accumulation of viable

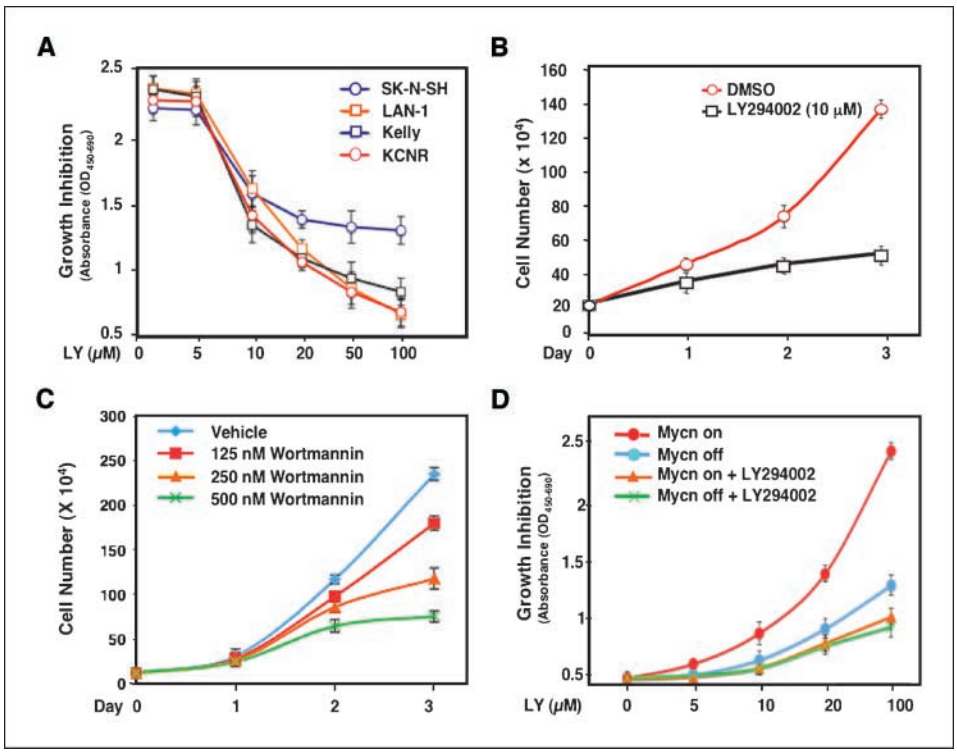

Figure 3. PI3K inhibition blocks accumulation of viable neuroblastoma cells. *A,* dose response of human neuroblastoma cell lines to PI3K inhibition. Neuroblastoma cell lines were treated with LY294002 at dosages shown and analyzed at 24 hours by water-soluble tetrazolium (WST-1) assay. SK-N-SH cells are diploid for *MYCN.* The other cell lines show amplification of *MYCN. B* and *C,* PI3K inhibition leads to decreased viability. The human neuroblastoma cell line Kelly was grown in the presence of LY294002 (*B*), wortmannin (*C*), or DMSO vehicle control. Wortmannin was added to medium twice daily. Viable trypan blue–excluding cells were counted on days shown. *D,* efficacy of PI3K-mediated proliferation block is dependent on Mycn. Tet21/N cells were treated with LY294002 or vehicle in the absence or presence of doxycycline. Decreased accumulation of viable cells mediated by LY294002 (hemacytometer counting) was most pronounced in cells that expressed *MYCN. A* to *D,* average of three separate experiments.

cells in the *MYCN*-amplified neuroblastoma cell lines LAN-1, Kelly, and KCNR (at 24 hours) in a dose-dependent manner (Fig. 3*A*). The inhibitory effects of LY294002 were pronounced in the two cell lines, showing amplification of *MYCN*, and were less prominent in the neuroblastoma line SK-N-SH, which is diploid for *MYCN* and expresses low levels of Mycn protein (Fig. 3*A*).

To address the effect of PI3K blockade over time (3 days), we studied the *MYCN*-amplified neuroblastoma cell line Kelly, which expresses high levels of Mycn. LY294002 treatment of Kelly cells led to decreased accumulation of viable cells in comparison with vehicle control (Fig. 3*B*). The PI3K inhibitor wortmannin had the same effect in a dose-dependent manner (Fig. 3*C*). Because wortmannin has a short half-life in tissue culture medium (25), inhibitory effects were observed only on dosing twice daily (Fig. 3*C*), a requirement that may explain why wortmannin dosed once daily failed to inhibit IGF-I-mediated induction of Mycn in long-term assays (26).

To further distinguish Mycn-dependent and Mycn-independent effects of PI3K inhibition, we analyzed Tet21/N cells, in which MYCN expression is controlled transcriptionally by the tetracycline system (19). In the absence of doxycycline, Tet21/N cells expressed high levels of Mycn (Fig. 3*D*) and showed increased accumulation of viable cells (Fig. 3*D, red curve*). Treatment of Mycn-expressing Tet21/N cells with LY294002 caused a marked decrease in accumulation of viable cells (Fig. 3*D, orange curve*). Doxycycline blocked transcription of Mycn (Fig. 3*D*), leading to decreased accumulation of viable cells, which was only slightly enhanced by LY294002 (Fig. 3*D*, compare *blue* and *green curves*). These data show that inhibition of PI3K is most effective in the presence of high levels of Mycn protein.

PI3K blockade induces apoptosis of neuroblastoma cells. Because apoptosis could contribute to the decreased accumulation of viable cells and because inhibition of PI3K may increase the susceptibility of neuroblastoma cells to apoptosis (27), we next

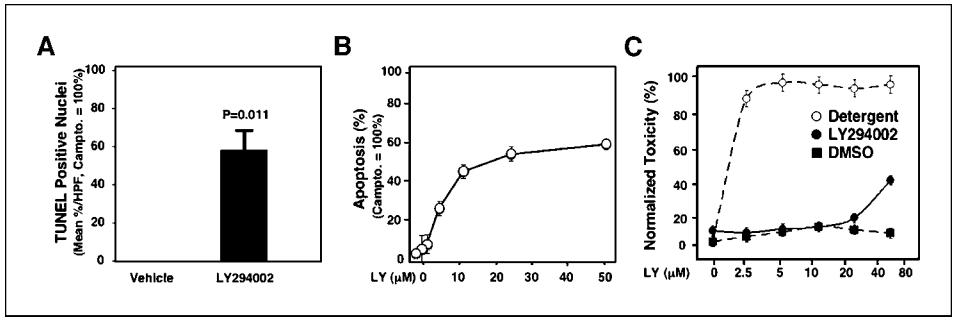

Figure 4. Inhibition of PI3K induces apoptosis of neuroblastoma cells. *A,* LAN-1 cells were treated with vehicle or LY294002 (10 μmol/L) for 24 hours. TUNEL-stained cells were visualized by confocal microscopy and quantitated (standardized to camptothecin = 100% apoptosis). *B,* as an independent measure of apoptosis, adherent LAN-1 neuroblastoma cells were examined by cell death detection ELISA at 24 hours as a function of LY294002 dosage. *C,* to assess toxicity of LY294002 treatment, Kelly cells were treated with LY294002 at doses indicated. DNA release into the culture medium was assessed at 24 hours using a dual-antibody ELISA to histone H2b to assay for cellular necrosis. Toxicity of LY294002 was detected above a dose of 25 μmol/L. Average of three separate experiments.

examined showed that inhibition of PI3K led to apoptosis. *MYCN*-amplified LAN-1 cells treated with LY294002 underwent a substantial increase in TUNEL positivity ($P = 0.011$), a measure of apoptosis (Fig. 4*A*). To confirm this result, we examined apoptosis using an ELISA that detected fragmented, nucleosomal DNA. This assay also showed increased levels of apoptosis as a function of LY294002 dosage (Fig. 4*B*). To exclude the possibility that nonspecific toxicity of LY294002 could be contributing to apoptosis or proliferation block, we did a histone H2b necrosis ELISA on adherent neuroblastoma cells after treatment with LY294002, showing nonspecific toxicity only at doses of LY294002 greater than 25 μmol/L (Fig. 4*C, solid circles* and *line*).

PI3K blockade activates GSK3β, leading to phosphorylation and destabilization of Mycn. Stabilization of Mycn protein may contribute to rapid progression in neuroblastoma tumors diploid for *MYCN* (28). Phosphorylation of Mycn represents an attractive mechanism through which tumor cells might stabilize Mycn, as during development of the cerebellum Mycn is phosphorylated by GSK3β and subsequently destabilized (29, 30). PI3K activates Akt, which in turn phosphorylates GSK3β, thereby negatively regulating its activity (31). Consistent with this model, Kelly neuroblastoma cells (grown in serum) showed high levels of pAkt and low levels of phosphorylated Mycn (pMycn). Subsequent treatment with LY294002 led to decreased levels of pAkt and increased levels of pMycn (Fig. 5*A*). We showed comparable results in the human neuroblastoma cell line SH-SY5Y (Fig. 5*B*). SH-SY5Y cells treated with IGF-I again showed high levels of pAkt, low levels of pMycn, and high levels of total Mycn. Treatment of these cells with the PI3K inhibitors LY294002 or wortmannin led to increased levels of pMycn and decreased levels of total Mycn (Fig. 5*B*).

To show that phosphorylation and stabilization of Mycn are mediated by the activity of GSK3β, we treated Kelly cells using a small-molecule inhibitor of GSK3β (30), which led to increased levels of Mycn (Fig. 5*C*). To clarify that the accumulation of Mycn protein resulted from decreased phosphorylation, we used a siRNA directed against GSK3β. siRNA treatment led to reduced levels of total GSK3β, a concomitant reduction in Mycn phosphorylation, and increased levels of total Mycn (Fig. 5*D*). Collectively, these data argue that blockade of PI3K signaling leads to phosphorylation and destabilization of Mycn in part through activating GSK3β.

Efficacy of PI3K blockade in neuroblastoma cells results primarily from Mycn phosphorylation, leading to destabilization. To assess the effect of LY294002 in a setting where *N-myc* phosphorylation (and destabilization) is not influenced by PI3K signaling, we transduced SHEP cells (in which Mycn is undetectable) with vector, wild-type *N-myc*, or the *N-myc* phosphorylation-deficient mutants *N-myc:T50A* (T50A) or *N-myc:S54A* (S54A). The stability of these proteins, which lack NH_2-terminal GSK3β phosphorylation sites, is not affected by PI3K activation or blockade (30).

SHEP lines expressing phosphorylated mutants of *N-myc* displayed enhanced growth in serum over several days (Fig. 6*A*). To clarify that this accumulation of viable cells was due to increased proliferation, we did a short-term BrdUrd incorporation assay. In this experiment, phosphorylated mutants of N-myc showed increased incorporation of BrdUrd and were resistant to the inhibitory effects of LY294002 (Fig. 6*B*). Treatment of vector-transduced SHEP cells with LY294002 led to a modest reduction in incorporation of BrdUrd. Transduction of wild-type *N-myc* led to increased of incorporation of BrdUrd (Fig. 6*B*). Subsequent

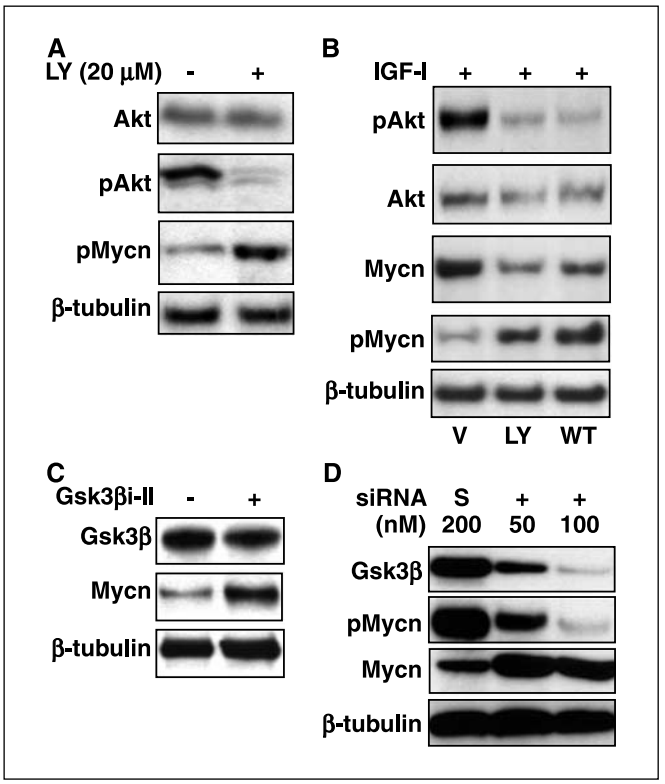

Figure 5. Inhibition of PI3K causes increased phosphorylation and decreased levels of Mycn protein. *A,* Kelly cells were treated with 20 μmol/L LY294002 for 24 hours in 10% serum, with lactacystin (10 μmol/L) added at 3 hours. Immunoblots show increased levels of pMycn and decreased levels of pAkt. *B,* serum-starved SH-SY5Y cells were treated for 6 hours with vehicle (*V*; DMSO), LY294002, or wortmannin in the presence of IGF-I and lactacystin. IGF-1 led to increased levels of pAkt. LY294002 and wortmannin blocked pAkt, resulting in increased levels of pMycn and decreased levels of total Mycn. *C,* chemical inhibition of GSK3β (SH-SY5Y cells, GSK inhibitor II) led to an increase in the level of total Mycn protein. *D,* siRNA-mediated inhibition of GSK3β leads to reduced levels of pMycn and increased levels of total Mycn, consistent with GSK3β as the kinase that directly phosphorylates and destabilizes Mycn. Kelly cells growing in serum were transiently transfected with siRNA directed against GSK3β or a scrambled siRNA control (*S*). Levels of GSK3β, pGSK3β, Mycn, and pMycn were assessed at 24 hours.

treatment of SHEP:*N-myc* cells with LY294002 caused a substantial decrease in proliferation to levels comparable with those in LY294002-treated cells transduced with vector alone.

SHEP cells transduced with T50A or S54A showed increased proliferation in comparison with wild-type *N-myc* and were resistant to the antiproliferative effects of LY294002. Importantly, SHEP cells expressing wild-type *N-myc* showed marked apoptosis in response to LY294002 treatment, suggesting induction of apoptosis as a significant mechanism contributing to the efficacy of LY294002-mediated blockade of *N-myc*. Phosphorylated mutants of *N-myc* were also less sensitive to the apoptosis-inducing effects of LY294002 (Fig. 6*C*). That phosphorylated specific mutants of *N-myc* are both proliferation proficient and apoptosis defective is consistent with recent observations describing an analogous phosphorylated mutant of *c-myc* (32). Although SHEP cells do not readily xenograft, we hypothesized that cells expressing phosphorylated mutants of *N-myc* might show increased efficiency of xenograft formation. Although initial xenograft tumor growth was more efficient for both phosphorylated mutants than it was for *N-myc*, none of these SHEP cell lines fully established as xenografts (data not shown).

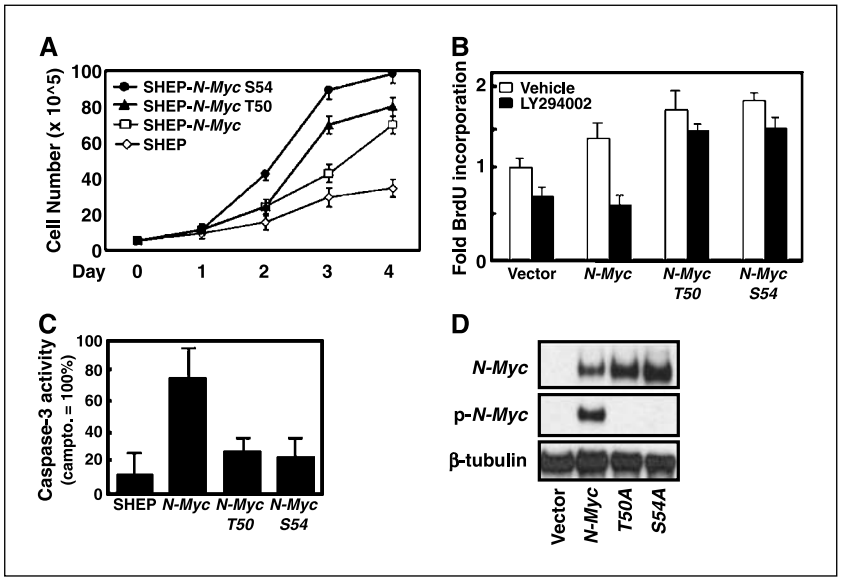

Figure 6. Nonphosphorylable mutants of *N-myc* are stabilized and resistant to PI3K inhibition. SHEP cells were stably transduced with wild-type *N-myc* or *N-myc* constructs mutant at the NH_2-terminal GSK3β phosphorylation sites. *A* to *C*, SHEP cells stably transduced with phosphorylation-defective mutants of *N-myc* grew more efficiently in the presence of serum (hemacytometer counting assay; *A*), incorporated more BrdUrd in the presence and absence of LY294002 (*B*), and were resistant to the proapoptotic effects of LY294002 (caspase-3 cleavage assay; *C*) in comparison with cells transduced with wild-type *N-myc*. *D*, Western analysis shows higher levels of *N-myc:T50A* and *N-myc:S54A* in contrast to wild-type *N-myc* protein. The two mutant *N-myc* proteins were also not phosphorylated appreciably (using antisera that recognizes both phosphorylation sites in *N-myc*; ref. 30).

Data presented in Fig. 6*A* to *C* suggest that phosphorylated mutants of *N-myc* showed increased stability compared with wild-type *N-myc* (even in the absence of PI3K inhibition) and that these mutant proteins were in addition resistant to degradation mediated by LY294002. To validate these observations biochemically, we did immunoblots, showing that SHEP cell lines harboring stably expressed *N-myc* phosphorylated mutants expressed higher total levels of *N-myc* and reduced levels of phosphorylated *N-myc* in comparison with wild-type *N-myc* protein (Fig. 6*D*).

PI3K blockade reduces the half-life of Mycn protein. To directly address the effect of PI3K inhibition on the stability of Mycn protein and the role of the T50 and S54 phosphorylated residues in this process, we tested the stability of wild-type and phosphorylated mutant myc proteins using cycloheximide to assess protein half-life in the absence of new protein synthesis. First, we showed that treatment with LY294002 led to a decrease in the half-life of Mycn protein (Fig. 7*A*). Kelly cells were grown in the presence of 10% FBS and were pretreated with LY294002 (20 μmol/L) or vehicle for 24 hours. Cells were then treated with cycloheximide and harvested at the time points shown (after cycloheximide). In control cells (no LY294002), Mycn protein was undetectable 4 hours after addition of cycloheximide ($t_{1/2}$, 2.3 hours). In cells treated with LY294002, Mycn was rapidly degraded and was undetectable 2 hours after addition of cycloheximide ($t_{1/2}$, 1.2 hours). These data show that blockade of PI3K led to a reduction in the half-life of wild-type Mycn protein, although it remains possible that other mechanisms also contributed to the decreased levels of Mycn seen in LY294002-treated cells (Fig. 2*A*).

Next, to verify that destabilization depends on phosphorylation at T50A and S54A, we compared the half-life of *N-myc, N-myc:T50A*, and *N-myc:S54A* proteins stably expressed in SHEP cells and treated with LY294002 for 24 hours before the addition of cycloheximide (Fig. 7*B*). In comparison with wild-type *N-myc*, both mutants were profoundly resistant to the destabilizing effects of LY294002 ($t_{1/2}$, *N-myc*, 1.2 hours; *N-myc:T50A*, 6.5 hours;

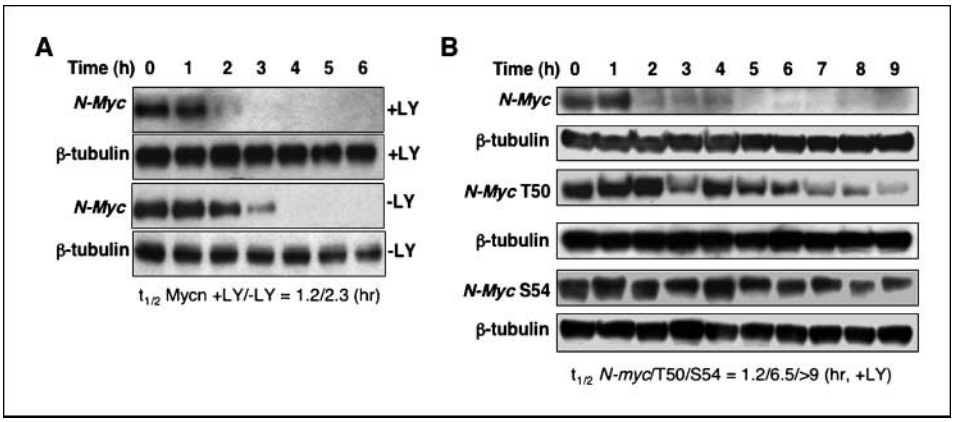

Figure 7. PI3K blockade reduces the half-life of Mycn protein. *A*, treatment of Kelly cells with cycloheximide verifies that LY294002 acts post-transcriptionally to destabilize Mycn protein. Cells were treated with 20 μmol/L LY294002 or vehicle for 24 hours before the addition of cycloheximide. LY294002 treatment led to rapid degradation of Mycn ($t_{1/2}$, 1.2 hours) compared with untreated controls ($t_{1/2}$, 2.3 hours). *B*, treatment of SHEP cells with cycloheximide verifies that phosphorylation-defective *N-myc* proteins show increased stability in the presence of LY294002. Cells were treated with as in (*A*) and harvested at the times shown (after cycloheximide addition). LY294002 treatment led to rapid degradation of *N-myc* to levels comparable with that in (*A*) ($t_{1/2}$, 1.2 hours). Phosphorylation-defective mutants of *N-myc* were stabilized dramatically, with half-lives 6.5 hours for the T50 mutant and >9 hours for the S54 mutant proteins. See Materials and Methods for details.

N-myc:S54, >9 hours). Collectively, these data argue that the effect of LY294002 treatment on *MYCN*-driven neuroblastoma proceeds primarily through phosphorylation and subsequent destabilization of Mycn protein.

Discussion

In this report, we show that PI3K inhibition represents an effective preclinical therapy for neuroblastoma and that the efficacy of this therapy occurs in part through destabilization of Mycn protein. Although PI3K inhibitors potentially act through both Mycn-dependent and Mycn-independent pathways, we provide several lines of evidence, indicating that degradation of Mycn represents a key target of PI3K inhibition. First, we showed that PI3K inhibition in murine neuroblastoma driven by a *MYCN* transgene led to decreased tumor mass and decreased levels of Mycn protein without significantly affecting levels of MYCN mRNA. Second, we showed that LY294002 therapy was most effective in human neuroblastoma cell lines with high levels of Mycn even when comparing isogenic cell lines that differed only in levels of expression of Mycn. Finally, we transduced human neuroblastoma cells with alleles of *N-myc* that could not be phosphorylated and degraded in response to PI3K inhibition. The efficacy of PI3K inhibition was dramatically reduced in these phosphorylation-defective mutants and was associated with marked stabilization of Mycn protein. Collectively, these data suggest that Mycn protein represents a critical therapeutic target in neuroblastoma cells treated with PI3K inhibitors.

Amplification of *MYCN* contributes prominently to neuroblastoma, is a strong independent predictor of poor patient outcome, and is therefore used to guide therapeutic decisions (6, 33–36). Although a large body of data supports a role for *MYCN* in the pathogenesis of neuroblastoma, few reports address the validity of Mycn protein as a therapeutic target in this disease. Inhibition of MYCN mRNA by antisense oligonucleotides (37–39) or as one effect of retinoic acid treatment (10) blocked proliferation and induced differentiation in neuroblastoma cells *in vitro*. Continuous delivery of antisense oligonucleotides against MYCN mRNA blocked development of tumors in mice transgenic for TH-*MYCN*. Our results extend these observations by showing that Mycn protein represents an important target for therapy of established neuroblastoma tumors *in vivo*.

The PI3Ks represent a diverse group of proteins. There are eight mammalian PI3Ks in three classes. All of these contain a catalytic p110 subunit, which in most cases heterodimerizes with a regulatory p85 subunit (reviewed in ref. 40). The small-molecule p110 inhibitors LY294002 and wortmannin have been critical to our current understanding of PI3K signaling (41, 42) and have been the only tools available to analyze this pathway over the past 10 years. As a consequence of inhibiting all known PI3Ks and a large number of related proteins, LY294002 and wortmannin show significant toxicity. Although it would be interesting to test the effect of small-molecule inhibitors of specific PI3K isoforms in this work, to more rigorously exclude nonspecific effects of drugs, such as LY294002, such reagents are only now becoming available. Several newer PI3K inhibitors that block specific isoforms of p110 should be better tolerated clinically and are now being developed and tested (43). The characterization of these molecules and the effect they have on different types of cancer should ensure the application of this promising therapeutic approach to patients with malignancies driven by PI3K activation.

The apparent stabilization of transcription factors through PI3K and downstream mediators affects a growing number of transcription factors, including β-catenin, Snail, Bcl-3, c-myc, and Mycn (30, 44–49). That all of these transcription factors play a role in malignant progression of specific cancers suggests that PI3K activation may use a common GSK3β-dependent mechanism to stabilize and thereby activate distinct transcriptional programs in different malignancies (37). Our studies complement earlier work showing that activation of Ras signaling also affected the GSK3β-mediated stabilization of c-myc and Mycn proteins (49–51). Importantly, these observations further suggest that inhibition of a single therapeutic target (PI3K) may be effective in a wide range of malignancies. The efficacy of PI3K inhibition presumably acts through blockade of transcriptional and cell cycle regulatory programs that may be unique to each cancer but are regulated by a common mechanism. The application of this therapy to children with neuroblastoma represents a promising approach to this common and generally lethal neoplasm.

Acknowledgments

Received 8/4/2005; revised 4/24/2006; accepted 6/1/2006.

Grant support: NIH grants K08NS053530-01A2 and RO1CAA102321, Thrasher Research Fund 2821-6, Sandler and Campini Families, and Waxman Foundation.

The costs of publication of this article were defrayed in part by the payment of page charges. This article must therefore be hereby marked *advertisement* in accordance with 18 U.S.C. Section 1734 solely to indicate this fact.

We thank Yun Bao and Qi-Wen Fan for experimental advice, David Ginzinger, Julie Weng, and Mamie Yu for assistance with quantitative RT-PCR analyses, Jane Gordon for assistance with confocal microscopy, Pat Reynolds and Jason Shohet for cell lines, and Gabriele Bergers and Chris Hackett for critical review of the article.

References

1. Brodeur GM. Neuroblastoma: biological insights into a clinical enigma. Nat Rev Cancer 2003;3:203–16.
2. Brodeur GM, Maris JM. Neuroblastoma. 4th ed. In: Pizzo PA, Poplack DG, editors. Principles and practice of pediatric oncology. Philadelphia: J.B. Lippincott Company; 2002. p. 895–938.
3. DuBois SG, Kalika Y, Lukens JN, et al. Metastatic sites in stage IV and IVS neuroblastoma correlate with age, tumor biology, and survival. J Pediatr Hematol Oncol 1999;21:181–9.
4. Norris MD, Bordow SB, Marshall GM, et al. Expression of the gene for multidrug-resistance-associated protein and outcome in patients with neuroblastoma. N Engl J Med 1996;334:231–8.
5. Brodeur GM, Seeger RC, Schwab M, Varmus HE, Bishop JM. Amplification of N-myc sequences in primary human neuroblastomas: correlation with advanced disease stage. Prog Clin Biol Res 1985;175:105–13.
6. Seeger RC, Brodeur GM, Sather H, et al. Association of multiple copies of the N-myc oncogene with rapid progression of neuroblastomas. N Engl J Med 1985;313:1111–6.
7. Meitar D, Crawford SE, Rademaker AW, Cohn SL. Tumor angiogenesis correlates with metastatic disease, N-Myc amplification, and poor outcome in human neuroblastoma. J Clin Oncol 1996;14:405–14.
8. Schweigerer L, Breit S, Wenzel A, et al. Augmented MYCN expression advances the malignant phenotype of human neuroblastoma cells: evidence for induction of autocrine growth factor activity. Cancer Res 1990;50:4411–6.
9. Breit S, Ashman K, Wilting J, et al. The N-myc oncogene in human neuroblastoma cells: down-regulation of an angiogenesis inhibitor identified as activin A. Cancer Res 2000;60:4596–601.
10. Thiele CJ, Reynolds CP, Israel MA. Decreased expression of N-myc precedes retinoic acid-induced morphological differentiation of human neuroblastoma. Nature 1985;313:404–6.
11. Hatzi E, Breit S, Zoephel A, et al. MYCN oncogene and angiogenesis: down-regulation of endothelial growth inhibitors in human neuroblastoma cells. Purification, structural, and functional characterization. Adv Exp Med Biol 2000;476:239–48.
12. Goodman LA, Liu BC, Thiele CJ, et al. Modulation of N-myc expression alters the invasiveness of neuroblastoma. Clin Exp Metastasis 1997;15:130–9.
13. Weiss WA, Aldape K, Mohapatra G, Feuerstein BG, Bishop JM. Targeted expression of MYCN causes neuroblastoma in transgenic mice. EMBO J 1997;16:2985–95.

14. Weiss WA, Godfrey T, Francisco C, Bishop JM. Genome-wide screen for allelic imbalance in a mouse model for neuroblastoma. Cancer Res 2000;60:2483–7.
15. Hackett CS, Hodgson JG, Law ME, et al. Genome-wide array CGH analysis of murine neuroblastoma reveals distinct genomic aberrations which parallel those in human tumors. Cancer Res 2003;63:5266–73.
16. Zimmerman KA, Yancopoulos GD, Collum RG, et al. Differential expression of myc family genes during murine development. Nature 1986;319:780–3.
17. Semsei I, Ma SY, Cutler RG. Tissue and age specific expression of the myc proto-oncogene family throughout the life span of the C57BL/6J mouse strain. Oncogene 1989;4:465–71.
18. Stanton BR, Parada LF. The N-myc proto-oncogene: developmental expression and *in vivo* site-directed mutagenesis. Brain Pathol 1992;2:71–83.
19. Lutz W, Stohr M, Schurmann J, et al. Conditional expression of N-myc in human neuroblastoma cells increases expression of α-prothymosin and ornithine decarboxylase and accelerates progression into S-phase early after mitogenic stimulation of quiescent cells. Oncogene 1996;13:803–12.
20. Cohn SL, London WB, Huang D, et al. MYCN expression is not prognostic of adverse outcome in advanced-stage neuroblastoma with nonamplified MYCN. J Clin Oncol 2000;18:3604–13.
21. Martin DM, Feldman EL. Regulation of insulin-like growth factor-IL expression and its role in autocrine growth of human neuroblastoma cells. J Cell Physiol 1993;155:290–300.
22. Misawa A, Hosoi H, Arimoto A, et al. N-Myc induction stimulated by insulin-like growth factor I through mitogen-activated protein kinase signaling pathway in human neuroblastoma cells. Cancer Res 2000;60:64–9.
23. Slack A, Chen Z, Tonelli R, et al. The p53 regulatory gene MDM2 is a direct transcriptional target of MYCN in neuroblastoma. Proc Natl Acad Sci U S A 2005;102:731–6.
24. Shohet JM, Hicks MJ, Plon SE, et al. Minichromosome maintenance protein MCM7 is a direct target of the MYCN transcription factor in neuroblastoma. Cancer Res 2002;62:1123–8.
25. Holleran JL, Egorin MJ, Zuhowski EG, et al. Use of high-performance liquid chromatography to characterize the rapid decomposition of wortmannin in tissue culture media. Anal Biochem 2003;323:19–25.
26. Misawa A, Hosoi H, Tsuchiya K, Sugimoto T. Rapamycin inhibits proliferation of human neuroblastoma cells without suppression of MycN. Int J Cancer 2003;104:233–7.
27. Kim S, Kang J, Qiao J, et al. Phosphatidylinositol 3-kinase inhibition down-regulates survivin and facilitates TRAIL-mediated apoptosis in neuroblastomas. J Pediatr Surg 2004;39:516–21.
28. Cohn SL, Salwen H, Quasney MW, et al. Prolonged N-myc protein half-life in a neuroblastoma cell line lacking N-myc amplification. Oncogene 1990;5:1821–7.
29. Kenney AM, Cole MD, Rowitch DH. Nmyc upregulation by sonic hedgehog signaling promotes proliferation in developing cerebellar granule neuron precursors. Development 2003;130:15–28.
30. Kenney AM, Widlund HR, Rowitch DH. Hedgehog and PI-3 kinase signaling converge on Nmyc1 to promote cell cycle progression in cerebellar neuronal precursors. Development 2004;131:217–28.
31. Cross DA, Alessi DR, Cohen P, Andjelkovich M, Hemmings BA. Inhibition of glycogen synthase kinase-3 by insulin mediated by protein kinase B. Nature 1995;378:785–9.
32. Hemann MT, Bric A, Teruya-Feldstein J, et al. Evasion of the p53 tumour surveillance network by tumour-derived MYC mutants. Nature 2005;436:807–11.
33. Brodeur GM, Seeger RC, Schwab M, Varmus HE, Bishop JM. Amplification of N-myc in untreated human neuroblastomas correlates with advanced disease stage. Science 1984;224:1121–4.
34. Matthay KK, Villablanca JG, Seeger RC, et al.; Children's Cancer Group. Treatment of high-risk neuroblastoma with intensive chemotherapy, radiotherapy, autologous bone marrow transplantation, and 13-*cis*-retinoic acid. N England Journal of Medicine 1999;341:1165–73.
35. Maris JM, Matthay KK. Molecular biology of neuroblastoma. J Clin Oncol 1999;17:2264–79.
36. Schmidt ML, Lukens JN, Seeger RC, et al. Biologic factors determine prognosis in infants with stage IV neuroblastoma: a prospective Children's Cancer Group study. J Clin Oncol 2000;18:1260–8.
37. Burkhart CA, Cheng AJ, Madafiglio J, et al. Effects of MYCN antisense oligonucleotide administration on tumorigenesis in a murine model of neuroblastoma. J Natl Cancer Inst 2003;95:1394–403.
38. Negroni A, Scarpa S, Romeo A, et al. Decrease of proliferation rate and induction of differentiation by a MYCN antisense DNA oligomer in a human neuroblastoma cell line. Cell Growth Differ 1991;2:511–8.
39. Schmidt ML, Salwen HR, Manohar CF, Ikegaki N, Cohn SL. The biological effects of antisense N-myc expression in human neuroblastoma. Cell Growth Differ 1994;5:171–8.
40. Wymann MP, Zvelebil M, Laffargue M. Phosphoinositide 3-kinase signalling—which way to target? Trends Pharmacol Sci 2003;24:366–76.
41. Yano H, Nakanishi S, Kimura K, et al. Inhibition of histamine secretion by wortmannin through the blockade of phosphatidylinositol 3-kinase in RBL-2H3 cells. J Biol Chem 1993;268:25846–56.
42. Vlahos CJ, Matter WF, Hui KY, Brown RF. A specific inhibitor of phosphatidylinositol 3-kinase, 2-(4-morpholinyl)-8-phenyl-4H-1-benzopyran-4-one (LY294002). J Biol Chem 1994;269:5241–8.
43. Knight ZA, Chiang GG, Alaimo PJ, et al. Isoform-specific phosphoinositide 3-kinase inhibitors from an arylmorpholine scaffold. Bioorg Med Chem 2004;12:4749–59.
44. Aberle H, Bauer A, Stappert J, Kispert A, Kemler R. β-Catenin is a target for the ubiquitin-proteasome pathway. EMBO J 1997;16:3797–804.
45. Zhou BP, Deng J, Xia W, et al. Dual regulation of Snail by GSK-3β-mediated phosphorylation in control of epithelial-mesenchymal transition. Nat Cell Biol 2004;6:931–40.
46. Viatour P, Dejardin E, Warnier M, et al. GSK3-mediated BCL-3 phosphorylation modulates its degradation and its oncogenicity. Mol Cell 2004;16:35–45.
47. Gregory MA, Hann SR. c-Myc proteolysis by the ubiquitin-proteasome pathway: stabilization of c-Myc in Burkitt's lymphoma cells. Mol Cell Biol 2000;20:2423–35.
48. Gregory MA, Qi Y, Hann SR. Phosphorylation by glycogen synthase kinase-3 controls c-myc proteolysis and subnuclear localization. J Biol Chem 2003;278:51606–12.
49. Yeh E, Cunningham M, Arnold H, et al. A signalling pathway controlling c-Myc degradation that impacts oncogenic transformation of human cells. Nat Cell Biol 2004;6:308–18.
50. Yaari S, Jacob-Hirsch J, Amariglio N, et al. Disruption of cooperation between Ras and MycN in human neuroblastoma cells promotes growth arrest. Clin Cancer Res 2005;11:4321–30.
51. Sears RC. The life cycle of C-myc: from synthesis to degradation. Cell Cycle 2004;3:1133–7.

Inhibition of PI3K Destabilizes Mycn

In the article on how inhibition of PI3K destabilizes Mycn in the August 15, 2006 issue of *Cancer Research* (1), there is an error in the order of authors. Dr. David D. Goldenberg and Dr. Chris Schlieve should be listed as the second and third authors, respectively.

1. Chesler L, Goldenberg DD, Schlieve C, Kenney A, Kim G, McMillan A, Matthay KK, Rowitch D, Weiss WA. Inhibition of phosphatidylinositol 3-kinase destabilizes Mycn protein and blocks malignant progression in neuroblastoma. Cancer Res 2006;66: 8139–46.

doi:10.1158/0008-5472.CAN-66-20-COR

Inhibition of Phosphatidylinositol 3-Kinase Destabilizes Mycn Protein and Blocks Malignant Progression in Neuroblastoma

Louis Chesler, Chris Schlieve, David D. Goldenberg, et al.

Cancer Res 2006;66:8139-8146.